

# Pinning of spiral fluxons by giant screw dislocations in $\text{YBa}_2\text{Cu}_3\text{O}_{7-\delta}$ single crystals: Josephson analog of the fishtail effect

S. Sergeenkov<sup>+</sup>, L. Jr. Cichetto<sup>+</sup>, V. A. G. Rivera<sup>+</sup>, C. Stari<sup>+\*</sup>, E. Marega<sup>∇</sup>, C. A. Cardoso<sup>+</sup>,  
F. M. Araujo-Moreira<sup>+1)</sup>

<sup>+</sup>Departamento de Física e Engenharia Física, Grupo de Materiais e Dispositivos, Centro Multidisciplinar para o Desenvolvimento de Materiais Cerâmicos, Universidade Federal de São Carlos, São Carlos, SP, 13565-905 Brazil

<sup>\*</sup>Instituto de Física, Facultad de Ingeniería, Julio Herrera y Reissig 565, C.C. 30, 11000 Montevideo, Uruguay

<sup>∇</sup>Instituto de Física, USP, São Carlos, SP, 13560-970 Brazil

Submitted 31 August 2009

Resubmitted 1 December 2009

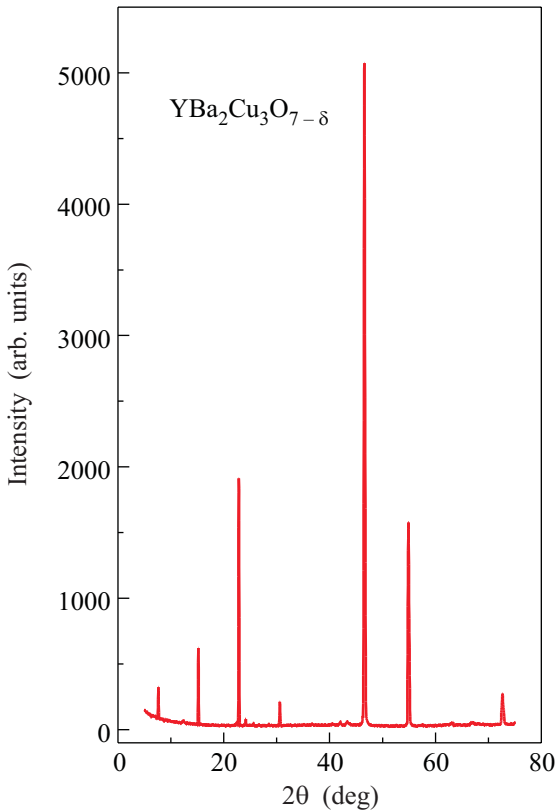
By using a highly sensitive homemade AC magnetic susceptibility technique, the magnetic flux penetration has been measured in  $\text{YBa}_2\text{Cu}_3\text{O}_{7-\delta}$  single crystals with giant screw dislocations (having the structure of the Archimedean spirals) exhibiting  $a = 3$  spiral turnings, the pitch  $b = 18.7 \mu\text{m}$  and the step height  $c = 1.2 \text{ nm}$  (the last parameter is responsible for creation of extended weak-link structure around the giant defects). The magnetic field applied parallel to the surface enters winding around the weak-link regions of the screw in the form of the so-called spiral Josephson fluxons characterized by the temperature dependent pitch  $b_f(T)$ . For a given temperature, a stabilization of the fluxon structure occurs when  $b_f(T)$  matches  $b$  (meaning an optimal pinning by the screw dislocations) and manifests itself as a pronounced low-field peak in the dependence of the susceptibility on magnetic field (applied normally to the surface) in the form resembling the high-field (Abrikosov) fishtail effect.

**1. Introduction.** Probably one of the most intriguing phenomena in the vast area of superconductivity is the so-called fishtail effect (FE) which manifests itself as a maximum in the field dependence of the magnetization. There are many different explanations regarding the existence and evolution of FE (see, e.g., [1–12] and further references therein). However, the most plausible scenario so far is based on the oxygen deficiency mediated pinning of Abrikosov vortices in non-stoichiometric materials with the highest possible  $T_C$  due to a perfect match between a vortex core and a defect size. It has been unambiguously demonstrated that by diminishing the deficiency of oxygen in undoped  $\text{YBa}_2\text{Cu}_3\text{O}_{7-\delta}$ , the FE decreases and tends to disappear completely. A characteristic field at which this phenomenon usually occurs is of the order of a few Tesla.

In this Letter we report on observation of a low-field (Josephson) analog of the high-field (Abrikosov) FE in  $\text{YBa}_2\text{Cu}_3\text{O}_{7-\delta}$  single crystals with giant screw dislocations (having the structure of Archimedean spirals), which we attributed to the perfectly matched pinning of the spiral 2D Josephson fluxons with the temperature dependent spiral pitch  $b_f(T)$  (predicted by Aranson, Gitterman, and Shapiro [13]) by the Archimedean spirals with the pitch  $b = 18.7 \mu\text{m}$ .

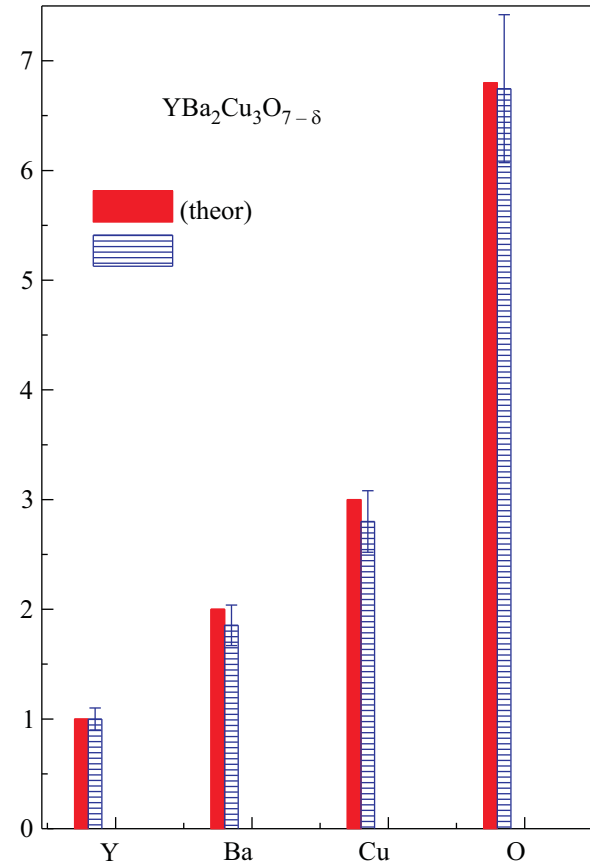
**2. Sample characterization.** One of the most reliable growing techniques used to obtain high-quality crystalline superconducting samples is related to the so-called chemical route based on the self-flux method [14]. It allows to obtain samples with almost no secondary phases (as compared to the traditional method of solid-state reaction [15]). Our samples ( $2.8 \times 2.1 \times 0.9 \text{ mm}^3$ ) were prepared following the self-flux method with different routes using both the heat treatment and environmental conditions (oxygen and argon atmospheres) [16]. The phase purity and the structural characteristics of our samples were confirmed by both scanning electron microscopy (SEM) with Energy Dispersive X-ray Analysis (EDX) accessory and X-ray diffraction (XRD), including the standard Rietveld analysis. Crystalline phases were confirmed by XRD using a Rigaku instrument with a Si 111 monochromator. XRD pattern (shown in Fig.1) was taken using  $\text{CuK}\alpha$  radiation ( $\lambda = 1.5418 \text{ \AA}$ ). Quantitative analysis of elements present in both crucibles and crystals was evaluated with accuracy of up to 0.01%. The resulting diagram is shown in Fig.2 which depicts the relative value of the components present in single crystal (normalized with respect to Y) along with the theoretically predicted estimates for  $\delta = 0.2$ . Fig.3 shows SEM surface scan topography of  $\text{YBa}_2\text{Cu}_3\text{O}_{7-\delta}$  single crystals with a giant screw dislocation having the structure of the Archimedean spi-

<sup>1)</sup>Research Leader, e-mail: faraujo@df.ufscar.br

Fig.1. XRD pattern of  $\text{YBa}_2\text{Cu}_3\text{O}_{7-\delta}$  single crystals

ral on  $100\ \mu\text{m}$  scale (with  $a = 3$  spiral turnings and the pitch  $b = 18.7\ \mu\text{m}$ ) along with a schematic structure of the one-armed Archimedean spiral (with three  $360^\circ$  turnings counterclockwise) which in polar coordinates is defined by the equation  $\rho = b\theta$  where  $b$  is a pitch (distance between successive turnings).

**3. Results and discussion.** AC susceptibility technique has proved very useful and versatile tool for probing low-field magnetic flux penetration in superconductors on macroscopic level (see, e.g., [17–21] and further references therein). In this paper, AC measurements were made by using a high-sensitivity homemade susceptometer based on the screening method and operating in the reflection configuration [17]. We have measured the complex AC susceptibility  $\chi_{ac} = \chi' + i\chi''$  as a function of the applied AC field  $h_{ac}(t) = h_0 \cos(\omega t)$  (with the amplitude  $0.01\ \text{Oe} \leq h_0 \leq 50\ \text{Oe}$  and frequency  $1\ \text{kHz} \leq \omega \leq 30\ \text{kHz}$ ) taken at fixed temperature. Initially, to ensure the formation of the so-called one-armed spiral fluxons [13] winding around the weak-link regions of the Archimedean spirals,  $h_{ac}$  was applied parallel to the sample's surface. To measure the response from the pinned (stabilized) fluxons, the magnetic field was applied normally to the surface. Fig.4 shows a typical dependence of the AC susceptibility  $\chi'(T, h_0)$  on AC

Fig.2. EDX spectrum of  $\text{YBa}_2\text{Cu}_3\text{O}_{7-\delta}$  single crystals prepared under argon atmosphere along with the theoretical value for each component (error bars are taken with the accuracy of  $\pm 10\%$ )

field amplitude  $h_0$  for different temperatures along with the corresponding critical temperature,  $T_C$ . It is important to notice that a rather high value of  $T_C$  in our single crystals is achieved by preparing samples in argon atmosphere. Notice an unusual reentrant-type behavior of  $\chi'(T, h_0)$  along with a clear peak-like structure (around  $h_0 = 5\ \text{Oe}$ ) shifting to lower fields with temperature (which indeed strongly resembles the high-field Abrikosov FE and by analogy will be called a low-field Josephson FE).

Turning to the discussion of the obtained results, let us show how the formation and pinning (by the Archimedean spirals) of spiral Josephson vortices (fluxons) can manifest itself as a pronounced low-field peak in the measured magnetic response. According to this scenario, the peak field  $h_p(T)$  (where susceptibility exhibits a fishtail-like low-field maximum) can be related to the fluxon critical field  $h_f(T) = \Phi_0/db_f$ . The latter defines the onset for fluxon motion. More precisely, for  $h_0 > h_f(T)$  spiral fluxons start to rotate along the weak-link regions of the Archimedean spirals. Here,

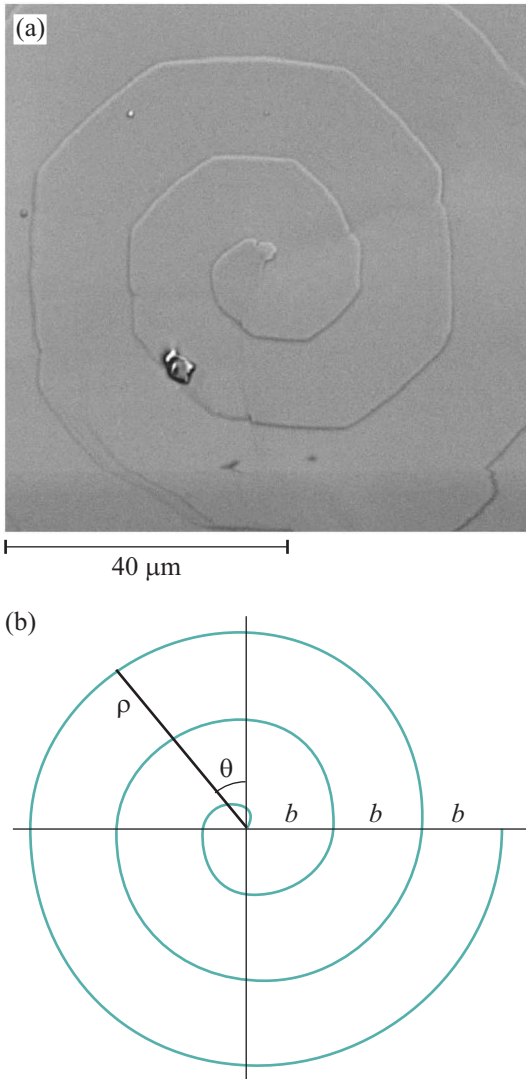


Fig.3. (a) SEM photograph of  $\text{YBa}_2\text{Cu}_3\text{O}_{7-\delta}$  single crystals showing a giant screw dislocation (having the structure of the Archimedean spiral) with  $a = 3$  spiral turnings and the pitch  $b = 18.7 \mu\text{m}$  (magnification 500 times). (b) Sketch of the one-armed Archimedean spiral with three  $360^\circ$  turnings (counterclockwise) in polar coordinates  $(\rho, \theta)$  and a pitch (distance between successive turnings)  $b$

$d = 2\lambda_L + c \simeq 2\lambda_L$  is the width of the contact with  $\lambda_L$  being the London penetration depth of the superconducting region and  $c$  the thickness of non-superconducting region in the vicinity of the screw defined by the vertical step height (distance between terraces of the screw dislocation along the  $c$ -axis of YBCO crystal). Typically [22],  $c$  is of the order of a unit cell (that is  $c \simeq 1.2 \text{ nm}$ ).  $b_f(T)$  is the temperature dependent pitch of the spiral Josephson vortex. According to the theoretical predictions [13],  $b_f(T) = 5\lambda_J(T)/\gamma(T)$ , where  $\lambda_J = \sqrt{\Phi_0/\mu_0 J_C d}$  is the Josephson penetration depth

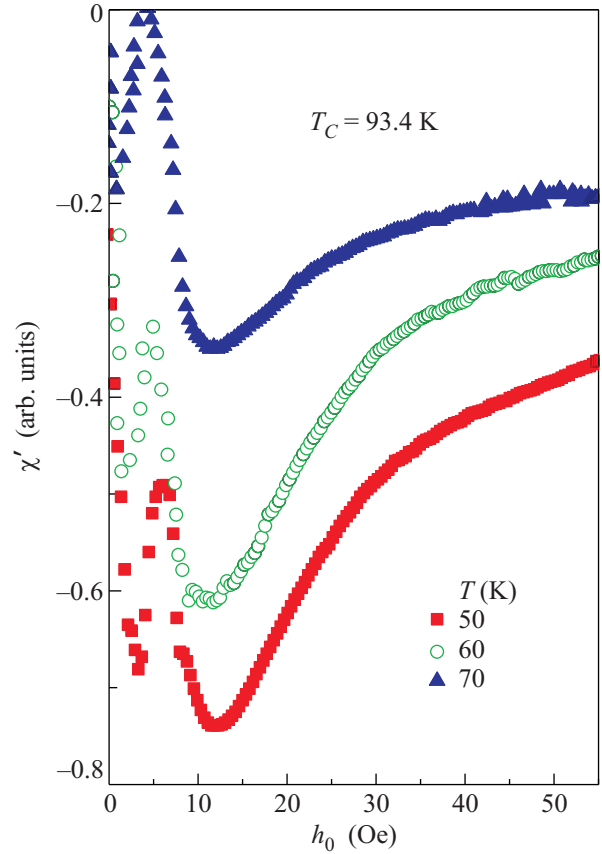


Fig.4. A fishtail-like structure of magnetic field dependence of the AC susceptibility  $\chi'(T, h_0)$  in  $\text{YBa}_2\text{Cu}_3\text{O}_{7-\delta}$  single crystals for various temperatures

(which also defines a size of the conventional 1D Josephson vortex and the lower Josephson field  $h_J = \Phi_0/\lambda_J d$ ) with  $J_C(T)$  being the critical current density; the temperature dependent factor  $\gamma(T)$  accounts for the onset border for spiral fluxon motion [13]. In our case,  $\gamma(T) = h_0/h_f(T) > 1$ . Recall [13] that the dynamics of the spiral fluxons is parametrically defined in polar coordinates as follows,  $x_f(t) = \rho \cos[n\theta(\rho) - \Omega t]$  and  $y_f(t) = \rho \sin[n\theta(\rho) - \Omega t]$  where  $n$  is the number of arms and  $\Omega$  is the angular velocity of fluxon rotation. In particular, for  $\theta(\rho) = \rho/b_f$ , the above relations describe the Archimedean spiral with pitch  $b_f$ . Above the critical field of the single spiral fluxon  $h_f(T)$ , the applied magnetic field first starts to penetrate the weakened regions (near the surface of the sample) which are situated in the vicinity of screw dislocations (see Fig.5, top). There are two possibilities depending on the field orientation. Flux can either enter by climbing up the screw dislocation from bottom to top (for field applied parallel to the surface) or by sliding down the screw from top to bottom (for field applied normally to the surface). In both cases, the freely rotating spiral fluxon eventually

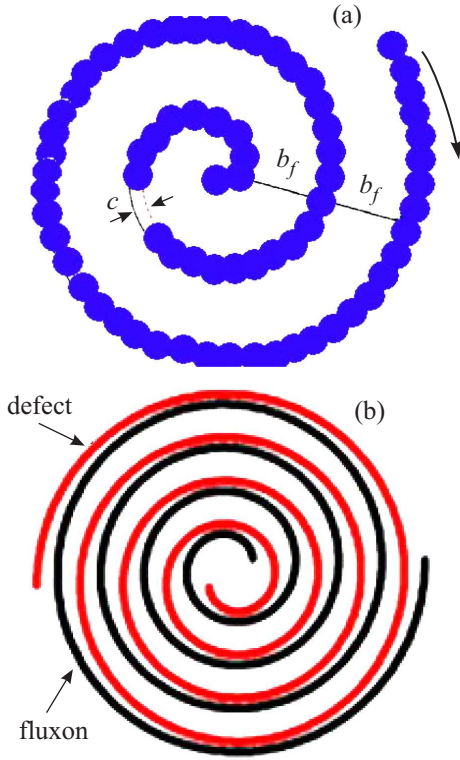


Fig.5. (a) The structure of the one-armed Josephson spiral fluxon with pitch  $b_f$  winding around the Archimedean spiral of the screw dislocation ( $c$  is distance between terraces along the  $c$ -axis of YBCO crystal). (b) Trapping (stabilization) of the one-armed Josephson spiral fluxon by the matching one-armed Archimedean spiral of the giant screw dislocation

gets trapped (stabilized) inside the Archimedean spiral of the defect (see Fig.5, bottom). To discuss the temperature evolution of the introduced parameters, in Fig.6 we present the fitting results for the temperature dependence of the normalized critical current density  $J_C(T)$  in our crystals, extracted from the AC susceptibility data using the usual procedure based on the critical state model [23]. A crossover between two different types of behavior is clearly seen near  $T^* = 0.8T_C$ . A low-temperature region ( $T < T^*$ ) was found to follow the well-known [24] two-fluid model dependence (solid line in Fig.6)  $J_C(T) = J_C(0)(1-t^4)^{3/2}$  with  $t = T/T_C$ , while closer to  $T_C$  (for  $T > T^*$ ) our data are better fitted by a proximity-type behavior [24] (dotted line in Fig.6)  $J_C(T) = J_C(0)(1-t^2)^2$ , most likely related to normal regions produced by oxygen deficiency and defect related structure. The extrapolated from the above fits zero-temperature value of the critical current density in our single crystals is  $J_C(0) = 5 \cdot 10^8$  A/m<sup>2</sup>. Assuming [24]  $\lambda_L(0) \simeq 100$  nm for the London penetration depth and using the above value of  $J_C(0)$ , we obtain  $\lambda_J(0) \simeq$

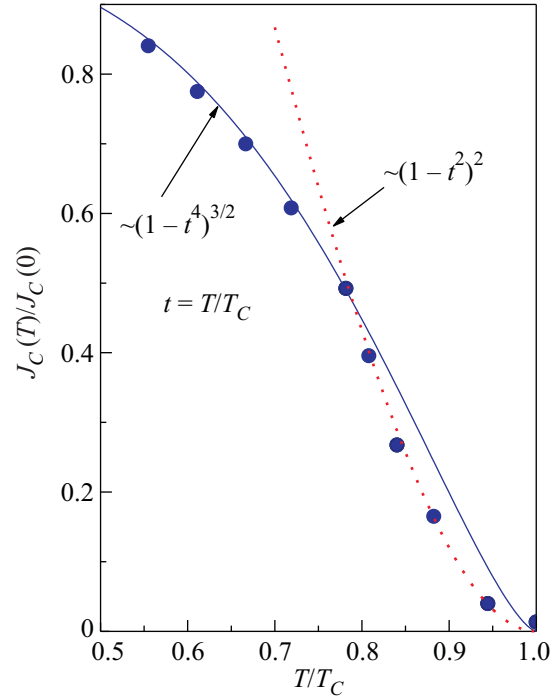


Fig.6. The best fits for the dependence of the normalized critical current density on reduced temperature  $T/T_C$  deduced from the AC susceptibility  $\chi'(T, h_0)$  data

$\simeq 3.6 \mu\text{m}$  for an estimate of zero-temperature Josephson penetration depth which in turn results in  $b_f(0) \simeq 18 \mu\text{m}/\gamma(0)$  and  $h_f(0) \simeq 5.5\gamma(0)$  Oe for the pitch of the spiral fluxon and the critical fluxon field, respectively. On the other hand, giant screw dislocations with a pronounced structure of Archimedean spiral (with the pitch  $b = 18.7 \mu\text{m}$ , see Fig.3), responsible for creation of Josephson contact areas  $S(T) = db = (2\lambda_L(T) + c)b \simeq 2\lambda_L(T)b$ , leads to the temperature dependence of the peak field  $h_p(T) = \Phi_0/S(T) \simeq \Phi_0/2\lambda_L(T)b$ . Using two-fluid model predictions for the explicit temperature dependence of the London penetration depth and critical current density,  $\lambda_L(T) = \lambda_L(0)/\sqrt{1-t^4}$  and  $J_C(T) = J_C(0)(1-t^4)^{3/2}$  with  $t = T/T_C$ , we obtain  $\lambda_J(T = 50 \text{ K}) \simeq 3.75 \mu\text{m}$ ,  $b_f(T = 50 \text{ K}) \simeq 18.75 \mu\text{m}/\gamma(T = 50 \text{ K})$ ,  $h_f(T = 50 \text{ K}) \simeq 5.33\gamma(T = 50 \text{ K})$  Oe, and  $h_p(T = 50 \text{ K}) \simeq 5.34$  Oe for the Josephson penetration depth, the pitch of the spiral fluxon, the critical fluxon field, and the peak field, respectively. Observe that for  $\gamma(T = 50 \text{ K}) \simeq 1.003$  we have a perfect match between the screw dislocation spiral pitch  $b$  (see Fig.3) and fluxon spiral pitch  $b_f(T = 50 \text{ K})$  leading to manifestation of the observed here low-field Josephson FE at  $h_p(T = 50 \text{ K}) \simeq h_f(T = 50 \text{ K})$ . Likewise, for higher temperatures the perfect match is achieved using  $\lambda_J(T = 60 \text{ K}) \simeq 3.95 \mu\text{m}$  and  $\lambda_J(T = 70 \text{ K}) \simeq$

$\simeq 4.4 \mu\text{m}$  for the Josephson penetration depth along with the two fitting parameters  $\gamma(T = 60 \text{ K}) \simeq 1.05$  and  $\gamma(T = 70 \text{ K}) \simeq 1.17$ . Besides, the above-obtained temperature dependence of the peak field  $h_p(T)$  correctly describes the observed slight shifting of the FE to lower applied fields with increasing the temperature (namely,  $h_p(T = 60 \text{ K}) \simeq 5.0 \text{ Oe}$  and  $h_p(T = 70 \text{ K}) \simeq 4.5 \text{ Oe}$ ). Notice also that, for the same temperatures, the lower Josephson field,  $h_J = \Phi_0/\lambda_J d$ , responsible for creation of conventional 1D vortices with the size of  $\lambda_J(T)$ , is too high to account for the observed low-field FE. Finally, let us estimate the pinning force density  $f_p$  for a spiral fluxon. By analogy with Abrikosov vortex core pinning by screw dislocations [5, 25], we obtain  $f_p \simeq (1/2)\mu_0 h_J^2 b_f \simeq 10^{-6} \text{ N/m}$  which, in the single vortex limit  $f_p = \Phi_0 J_C$ , corresponds to the maximum value of the critical current density  $J_C \simeq 5 \cdot 10^8 \text{ A/m}^2$  in our crystals.

In summary, employing a highly sensitive homemade AC magnetic susceptibility technique to single crystals of  $\text{YBa}_2\text{Cu}_3\text{O}_{7-\delta}$  with giant 3D screw dislocations (having the structure of the 2D Archimedean spiral), we observed a manifestation of the low-field analog of the high-field (Abrikosov) fishtail effect, attributed to highly efficient pinning (stabilization) of rotating spiral Josephson vortices by the matching screw defects.

This work has been financially supported by the Brazilian agencies CNPq, CAPES and FAPESP.

1. D. Daeumling, J. M. Seuntjens, and D. C. Larbalestier, *Nature* **346**, 332 (1990).
2. V. F. Gantmakher, A. M. Neminskii, and D. V. Shovkun, *JETP Lett.* **52**, 630 (1990).
3. G. Yang, P. Shang, S. D. Sutton et al., *Phys. Rev. B* **48**, 4054 (1993).
4. X. Y. Cai, A. Gurevich, D. C. Larbalestier et al., *Phys. Rev. B* **50**, 16774 (1994).
5. S. Sergeenkov, *J. Appl. Phys.* **78**, 1114 (1995).
6. I. M. Babich and G. P. Mikitik, *JETP Lett.* **64**, 586 (1996).
7. Y. Kopelevich and P. Esquinazi, *J. Low Temp. Phys.* **113**, 1 (1998).
8. W. A. C. Passos, P. N. Lisboa-Filho, R. Caparroz et al., *Physica C* **354**, 189 (2001).
9. I. M. Sutjahja, M. Diantoro, D. Darminto et al., *Physica C* **378**, 541 (2002).
10. S. Sergeenkov, *JETP Lett.* **77**, 99 (2003).
11. C. A. Cardoso and O. F. de Lima, *J. Appl. Phys.* **95**, 1301 (2004).
12. G. Pasquini and V. Bekkeris, *Supercond. Sci. Technol.* **19**, 671 (2006).
13. I. Aranson, M. Gitterman, and B. Ya. Shapiro, *Phys. Rev. B* **52**, 12878 (1995).
14. C. Changkang, *Prog. Crystal Growth and Charact.* **36**, 1 (1998).
15. M. Kakihana, *J. Sol-Gel Sci. Technol.* **6**, 7 (1996).
16. C. Stari, V. A. G. Rivera, A. J. C. Lanfredi et al., *J. Magn. Magn. Mater.* **320**, e504 (2008).
17. F. M. Araujo-Moreira, P. Barbara, A. Cawthorne, and C. J. Lobb, *Phys. Rev. Lett.* **78**, 4625 (1997).
18. S. Sergeenkov and F. M. Araujo-Moreira, *JETP Lett.* **80**, 580 (2004).
19. F. M. Araujo-Moreira and S. Sergeenkov, *Supercond. Sci. Technol.* **21**, 045002 (2008).
20. V. A. G. Rivera, S. Sergeenkov, C. Stari et al., *JETP Lett.* **90**, 365 (2009).
21. C. A. Cardoso, M. A. Avila, R. A. Ribeiro et al., *Physica C* **354**, 165 (2001).
22. C. Gerber, D. Anselmetti, J. G. Bednorz et al., *Nature* **350**, 279 (1991).
23. C. P. Bean, *Rev. Mod. Phys.* **36**, 39 (1964).
24. C. P. Poole, Jr., H. A. Farach, and R. J. Creswick, *Superconductivity*, Academic Press, New York, 1995.
25. M. McElfresh, T. G. Miller, D. M. Schaefer et al., *J. Appl. Phys.* **71**, 5099 (1992).